Octa-guanidine Morpholino Restores Dystrophin Expression in Cardiac and Skeletal Muscles and Ameliorates Pathology in Dystrophic *mdx* Mice

Bo Wu[1], Yongfu Li[2], Paul A Morcos[2], Timothy J Doran[1], Peijuan Lu[1] and Qi Long Lu[1]

[1]*Department of Neurology, McColl-Lockwood Laboratory for Muscular Dystrophy Laboratory, Neuromuscular/ALS Center, Carolinas Medical Center, Charlotte, North Carolina, USA;* [2]*Gene Tools, LLC, Philomath, Oregon, USA*

Steric-block antisense oligonucleotides (AONs) are able to target RNAs for destruction and splicing alteration. Reading frame restoration of the dystrophin transcript can be achieved by AON-mediated exon skipping in the dystrophic *mdx* mouse model. However, simple, unmodified AONs exhibit inefficient delivery systemically, leading to dystrophin induction with high variability in skeletal muscles and barely detectable in cardiac muscle. Here, we examined a Morpholino oligomer conjugated with a dendrimeric octaguanidine (Vivo-Morpholino) and demonstrated that the delivery moiety significantly improved dystrophin production in both skeletal and cardiac muscles in *mdx* mice *in vivo*. Single intravenous (IV) injections of 6 mg/kg Vivo-MorpholinoE23 (Vivo-ME23) generated dystrophin expression in skeletal muscles at the levels higher than the injection of 300 mg/kg unmodified ME23. Repeated injections at biweekly intervals achieved near 100% of fibers expressing dystrophin in skeletal muscles bodywide without eliciting a detectable immune response. Dystrophin protein was restored to ~50 and 10% of normal levels in skeletal and cardiac muscles, respectively. Vivo-Morpholinos showed no signs of toxicity with the effective dosages and regime, thus offering realistic prospects for the treatment of a majority of Duchenne muscular dystrophy (DMD) patients and many other diseases by targeting RNAs.

Received 3 September 2008; accepted 5 February 2009; published online 10 March 2009. doi:10.1038/mt.2009.38

INTRODUCTION

Antisense oligonucleotide (AON) therapy has been recently demonstrated with great potential for treating diseases from viral infections to cancers by knocking down the targeted transcripts.[1,2] Successful application of the therapy has now been extended for the treatment of Duchenne muscular dystrophy (DMD). This application uses sequence-specific AONs for targeted exon skipping to correct the reading frame of mutated dystrophin mRNA.[3–8] DMD presents an unparalleled prospect for gene correction by AONs therapy for two main reasons. First, the gene consists of 79 exons spanning >2.3 million base pairs. The muscle form of dystrophin protein, containing 3,685 amino acids (427 kd), can be divided into four structural domains: amino terminal, rod, cysteine-rich, and carboxy terminal. More important, the rod domain appears not to be critical for the functions of dystrophin. For instance, deletion of exons from 17 to 49 was associated with only a mild clinical phenotype.[9] Similarly, an artificially constructed microdystrophin with a deletion from exon 18 to 58 remains largely functional.[10] Second, a large proportion of DMD mutations occur within this noncritical rod region of the gene. Thus critical functions of the protein can be retained despite skipping of the mutated exon or of exons necessary for the restoration of open reading frame. It is estimated that AON therapy would be able to correct nearly all types of mutations in the rod region, transforming >60% DMD to near-normal phenotypes or to a milder Becker muscular dystrophy.[9,11,12] It is encouraging that dystrophin positive muscle fibers are found in many DMD muscles and in animal models of DMD. These so called revertant fibers appear to be the product of spontaneously altered splicing that skips the mutated exon or exons that disrupt the reading frame of the endogenous gene.[13] The presence of these revertant dystrophin proteins may provide a basis for the immune tolerance to the dystrophin induced by AONs.

The potential of AON-mediated exon skipping for the treatment of DMD was initially demonstrated in cell culture systems and in the dystrophic *mdx* mouse.[4,5] More recently, restoration of dystrophin expression by antisense therapy has been demonstrated in DMD patients via intramuscular injection of 2'O methyl phosphorothioate (2OMePS) AONs in the Netherlands.[14] However, exon skipping and dystrophin expression induced by all unmodified antisense chemistries are highly variable, and therapeutic amounts of dystrophin have been achieved only in some skeletal muscles through systemic delivery of Morpholino oligos.[15] Furthermore, effective dystrophin expression has not been achieved in the cardiac muscle when unmodified Morpholino oligos were used. This could severely reduce the therapeutic value of antisense therapy for treating DMD as the disease affects all body muscles, and fatality is commonly the direct consequences of the failure of respiratory and cardiac functions.[16,17]

One approach to improve the efficiency of exon skipping is to enhance the delivery efficiency of oligos by attaching them

Correspondence: *Qi Long Lu, McColl-Lockwood Laboratory for Muscular Dystrophy Laboratory, Neuromuscular/ALS Center, Carolinas Medical Center, 1000 Blythe Blvd, Charlotte, North Carolina 28231, USA. E-mail: qi.lu@carolinashealthcare.org*

to cell-penetrating peptides.[18,19] Most recently, we and other groups have shown high levels of dystrophin expression in both skeletal and cardiac muscles by Morpholinos tagged with specifically designed arginine-rich peptides.[19–21] However, long-term repeated applications of peptides required for treating DMD with antisense oligomers risk a potential immune response. Guanidinium head groups of arginine-rich peptides are principally responsible for effective delivery of Morpholino oligos[19] and 8–10 guanidine head groups exhibit the most efficient delivery enhancing effect.[22] Here, we report the use of a nonpeptide dendrimeric octaguanidine moiety–tagged morpholino oligomer targeting mouse dystrophin exon 23 (E23) [Vivo-MorpholinoE23 (Vivo-ME23)]. We demonstrated that the delivery moiety significantly improved efficiency of ME23-induced skipping of E23 in *mdx* mice, a model of human DMD. A single intravenous (IV) injection of 6 mg/kg Vivo-ME23 induced functional levels of dystrophin in bodywide skeletal muscles equivalent to that achieved by 300 mg/kg unmodified ME23. Repeated injections of Vivo-ME23 restored homogeneous expression of dystrophin in all skeletal muscles and partial expression in cardiac muscle without eliciting a detectable immune response. This together with the improvement of muscle pathology indicates the feasibility of the use of Vivo-Morpholino as antisense therapy for the treatment of a majority of DMD patients. Effective targeting for dystrophin expression was also demonstrated in smooth muscles of blood vessels bodywide. Conjugation of morpholinos with the nonpeptide delivery moiety, therefore, also provides promise for universal delivery of oligonucleotides to achieve RNA interference for treating diseases from viral infections to cancers.

RESULTS

Intramuscular injection of Vivo-ME23-induced dystrophin expression in >90% muscle fibers

The *mdx* mouse exhibits a nonsense-point mutation in E23 of the dystrophin gene and, except for a few revertant fibers or cardiomyocytes, produces no dystrophin in either skeletal or cardiac muscles.[5,6,23,24] Our previous studies have shown that a Morpholino oligomer, E23 + 7–18 (referred as ME23), targeting the boundary sequence of E23 (last seven bases) and intron 23 (first 18 bases) in the mouse dystrophin gene was able to induce skipping of E23 and dystrophin expression in muscles of the *mdx* mice.[15] However, restoration of functional amounts of dystrophin in muscles requires repeated injections of large amounts of ME23. Furthermore, dystrophin induction was highly variable within and between the skeletal muscles and was barely detectable in cardiac muscle. We suspect that the low efficiency of antisense effects is primarily due to the poor penetration of Morpholino into cells, severely limiting the amounts of AON gaining access to its intracellular target. To explore whether delivery-enabled Morpholino can improve antisense effects, we first compared the octa-guanidine-conjugated ME23 (Vivo-ME23) (**Figure 1a**) to the unmodified ME23 injected intramuscularly, either alone or with endoporter, an amphiphilic peptide (hereafter referred as ME23 + endoporter). All formulations of ME23 induced dystrophin expression in tibialis anterior (TA) muscles of adult (4–5 weeks) *mdx* mice (**Figure 1b**). The number of dystrophin-positive fibers was 61.80 ± 1.66% and 95.80 ± 1.16% with injection of 2 and 10 µg of the Vivo-ME23, respectively, significantly higher than those with unmodified ME23 (40.60 ± 0.93% and 63.20 ± 1.16%) and ME23 + endoporter (48.80 ± 1.59% and 71.80 ± 2.67%) (each group $n = 6$, t-test, $P < 0.05$) (**Figure 1c**). Consistently, dystrophin expression was more homogenous in the muscles treated with Vivo-ME23 at both dosages, whereas groups of dystrophin-negative fibers were often intermixed with dystrophin-positive fibers in muscles treated with the other ME23 formulations, particularly at the lower dosage (**Figure 1b**). The higher efficiency of Vivo-ME23 was also demonstrated by western blot (**Figure 1d**). No increased local muscle damage or mononucleate infiltration was observed (data not shown). These results suggest that Vivo-Morpholinos improve antisense effects without local toxicity.

Effective restoration of dystrophin expression in abdominal and diaphragm muscles by intraperitoneal injection of Vivo-ME23

Next, we examined the Vivo-ME23 for exon skipping systemically in the *mdx* mice by intraperitoneal (IP) injection, as this route of delivery has been reported to efficiently induce exon skipping throughout body tissues.[18] The mice were treated with a single IP injection of 6 mg/kg or 30 mg/kg of Vivo-ME23 (estimated from the effective dosage used in the intramuscular injection), and exon skipping and dystrophin induction were examined 2 weeks later. Dystrophin was clearly detected by immunohistochemistry in >40% of muscle fibers in both abdominal and diaphragm muscles after treatment of 6 mg/kg Vivo-ME23, especially the muscle fibers in the layers near the peritoneal surface of the abdomen. However, dystrophin was detected in <5% of fibers in all other skeletal muscles examined and not detected in the heart muscle (**Figure 2a,c**). The same amount of unmodified ME23, injected IP, induced <5% dystrophin-positive fibers in both abdominal and diaphragm muscles, and no increase in dystrophin-positive fibers in any other skeletal or cardiac muscles was observed (data not shown). Efficiency of dystrophin induction was further improved with a higher dose, 30 mg/kg Vivo-ME23. Nearly all muscle fibers were dystrophin positive in both diaphragm and abdominal muscles, including those in the deeper muscle layers (**Figure 2d**). The skipping of E23 in these tissues was confirmed by reverse transcriptase (RT)-PCR (**Figure 2f**). Expression of dystrophin in all other skeletal muscles remained at low levels with <15% of fibers being dystrophin positive. Again, no dystrophin-positive cardiomyocytes were detected in heart muscles, except for a few isolated revertant cardiomyocytes that were also seen in untreated *mdx* mice (**Figure 2d**, **Supplementary Figure S1**). These results suggest that IP administration provides significant local, but limited systemic antisense effect. This was further supported by the results from repeated IP injections. Administration of 15 mg/kg Vivo-ME23 every other day for 20 days induced dystrophin expression in all fibers of both diaphragm and abdominal muscles with an intensity of the staining similar to that seen in the normal control muscles of *C57B/6* mice (**Figure 2a,e**). However, <30% of dystrophin-positive fibers were seen in other skeletal muscles including biceps, TA, gastrocnemius, and quadriceps, and variations in the levels of dystrophin expression between fibers and muscles were apparent. Furthermore, in heart, convincing signals for dystrophin expression were detected in very few cardiomyocytes (<1%),

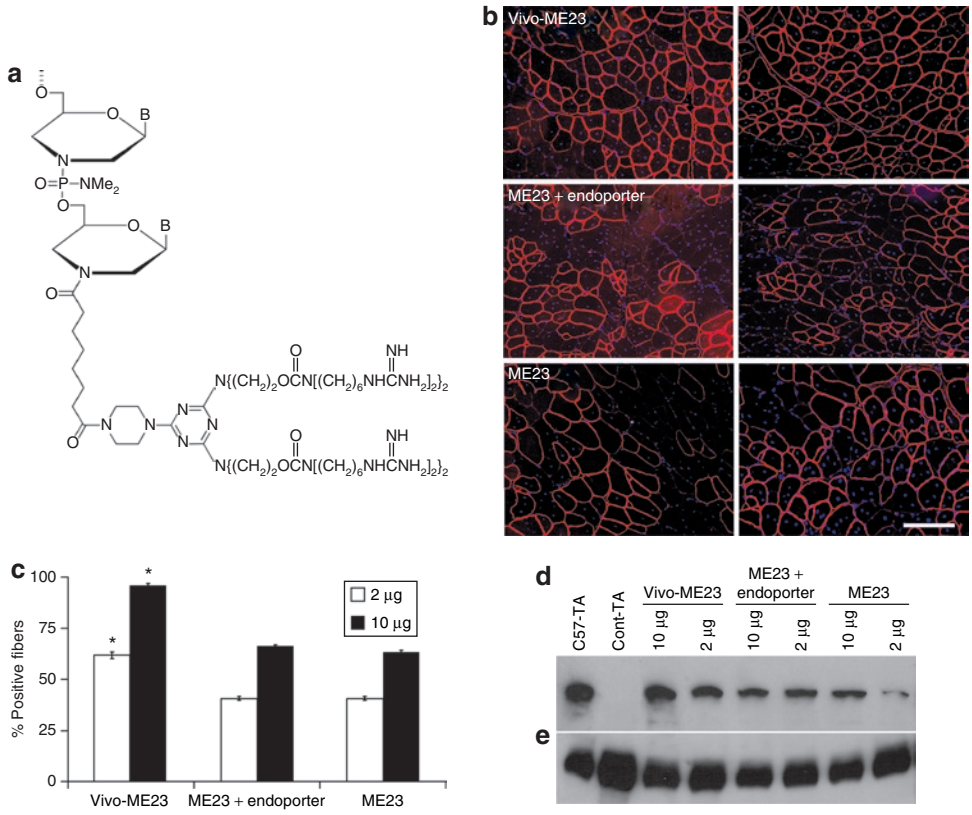

Figure 1 Chemical structure of Vivo-Morpholino and dystrophin expression after intramuscular injection of Morpholinos. (**a**) Structure of Vivo-Morpholino, a Morpholino oligo coupled with a dendrimeric octaguanidine moiety assembled from a triazine core with a guanidine head group at the end of each side chain. (**b–d**) Comparison of dystrophin induction in tibialis anterior (TA) muscles with Vivo-MorpholinoE23 (Vivo-ME23), MorpholinoE23 + endoporter (ME23 + endoporter), and MorpholinoE23 (ME23) by intramuscular injections. The muscles of adult *mdx* mice were injected with 2 µg (left column) or 10 µg (right column) of each oligomer. (**b**) Blue nuclear staining with 4′-6-Diamidino-2-phenylindole. Bar = 100 µm. (**c**) Maximum number dystrophin-positive fibers were counted in a single cross-section. $n = 6$ for each group, $P < 0.05$, *t*-test. (**d**) Western blot demonstrates dystrophin in the muscles detected with the NCL-DYS1 monoclonal antibody. C57-TA, TA muscles from normal *C57BL/6*; Cont-TA, TA muscle from untreated *mdx* mouse. (**e**) α-actin as loading controls.

although weak, patchy, membrane staining was present in a small proportion of the cells (**Figure 2e**). The marked disparity in the levels of dystrophin expression between diaphragm, heart, and other skeletal muscles was also confirmed by RT-PCR and western blots (**Figures 2f** and **3e**).

IV injection of Vivo-ME23 induced high level of dystrophin expression in all skeletal muscles

We then examined the systemic effects of the Vivo-ME23 by IV injections. Treating the *mdx* mice with single injection of 6 mg/kg Vivo-ME23 produced detectable dystrophin expression in >50% fibers of all skeletal muscles by immunohistochemistry 2 weeks after injection (**Figure 3a,c**; **Supplementary Figure S1**) with a significant reduction in serum levels of creatine kinase (**Figure 3f**). More important, strong dystrophin expression was clearly demonstrated in a considerable number of cardiomyocytes (up to 300 cardiomyocytes in a single cross-section of the heart) accompanied by weak, but identifiable staining for dystrophin in a large proportion of the remaining cardiac muscle (**Figure 3c**). In contrast, single IV injection of 300 mg/kg of unmodified ME23 produced <50% of dystrophin-positive fibers, a proportion of them weakly stained, in any skeletal muscle (**Figure 3b,d**; **Supplement Figure S1**). The number of cardiomyocytes with strong dystrophin expression in heart remained at levels similar to those in the untreated *mdx* mice (<20 cardiomyocytes in any cross-section of the heart), and no weak expression was detected in the remaining cardiomyocytes. The significantly higher efficiency of dystrophin induction with the Vivo-ME23 than unmodified ME23 was confirmed by western blots (**Figure 3e**).

Repeated IV injections restore dystrophin expression in nearly all skeletal muscle fibers

To investigate the potential cumulative effects of antisense therapy required for treating DMD, we injected 6 mg/kg of the Vivo-ME23 intravenously five times at biweekly intervals into adult *mdx* mice and examined muscles 2 weeks after the last injection. Nearly all fibers in all skeletal muscles, including diaphragm, intercostals, digital muscles, back trapezius, thoracic, and lumbar muscles expressed normal levels of dystrophin immunohistochemically, with weaker expression observed in only a small proportion of the fibers (<10%) (**Figure 4a**, **Supplementary Figure S1**). More important, dystrophin induction also increased significantly in the cardiac muscle, with >40% of the cardiomyocytes expressing clearly identifiable dystrophin, although considerable variation persisted between areas (**Figure 4b**, **Supplementary Figure S1**). Consistently, western blots revealed >50% of the normal levels of

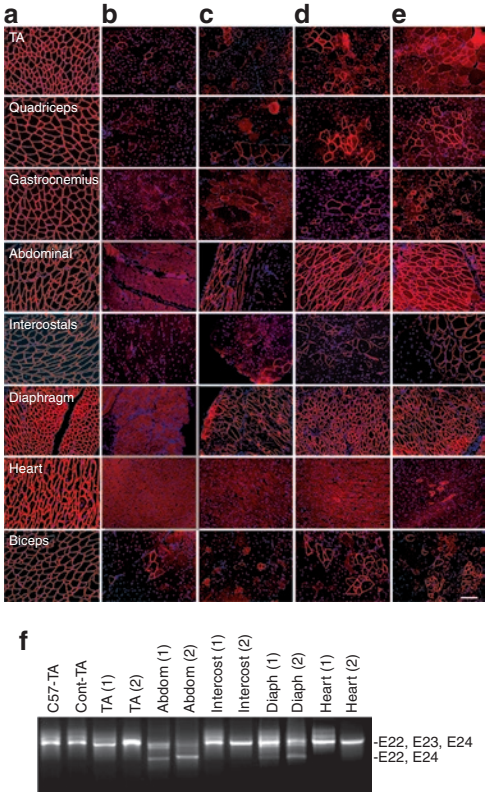

Figure 2 Restoration of dystrophin expression by intraperitoneal (IP) injection of Vivo-MorpholinoE23. Muscles from (**a**) normal *C57BL/6* mouse, (**b**) untreated *mdx* mouse, and (**c**) Vivo-MorpholinoE23-treated *mdx* mice with a single 6 mg/kg, (**d**) a single 30 mg/kg, and (**e**) 10 times 15 mg/kg injections, respectively. Blue nuclear staining with 4′-6-Diamidino-2-phenylindole. Bar = 100 µm. (**f**) Detection of exon 23 skipping in muscles by reverse transcriptase-PCR 2 weeks after the last injection. C57-TA, TA muscle from normal *C57BL/6* mouse; Cont-TA, TA muscle from untreated *mdx* mouse; Abdom, abdominals; Intercost, intercostals; Diaph, diaphragm. (1) and (2) represent muscles from mouse treated (IP) with single 30 mg/kg or 10 times 15 mg/kg of Vivo-MorpholinoE23, respectively. The upper 1,093-bp bands (indicated by E22, E23, E24) correspond to the normal dystrophin mRNA and the lower 880-bp bands (indicated by E22, E24) correspond to the mRNA with exon 23 skipped.

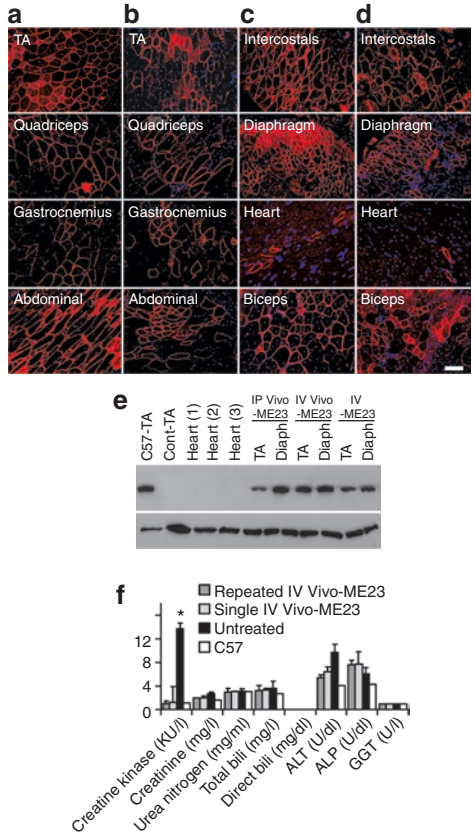

Figure 3 Restoration of dystrophin expression by single intravenous (IV) injection of morpholinos. (**a** and **c**) 6 mg/kg Vivo-MorpholinoE23 (Vivo-ME23). (**b** and **d**) 300 mg/kg MorpholinoE23. Blue nuclear staining with 4′-6-Diamidino-2-phenylindole. Bar = 50 µm. (**e**) Western blot shows the levels of dystrophin expression detected with the NCL-DYS1 monoclonal antibody (upper panel). Lower panel is α-actin as loading controls. C57-TA, TA muscle from normal C57BL/6 mouse (50% protein loading compared to the other samples); Cont-TA, TA muscle from untreated *mdx* mouse. Hearts correspond to cardiac muscles from *mdx* mice treated with 10 times intraperitoneal (IP) injections of 15 mg/kg Vivo-ME23 (1), single IV injection of 6 mg/kg Vivo-ME23 (2), and single IV injection of 300 mg/kg MorpholinoE23 (3). Diaph, diaphragm. Muscles from the *mdx* mice treated with 10 times IP injections of 15 mg/kg Vivo-ME23 (IP Vivo-ME23); single IV injection of 6 mg/kg Vivo-ME23 (IV Vivo-ME23); and single IV injection of 300 mg/kg MorpholinoE23 (IV-ME23), respectively. (**f**) The levels of serum enzymes. Repeated IV Vivo-ME23, single IV Vivo-ME23; Untreated, samples from untreated *mdx* mice; C57, C57BL/6 mouse. Creatine kinase (KU/l), creatinine (mg/l), urea nitrogen (mg/ml), total bilirubin (mg/l), direct bilirubin (mg/dl), alanine transaminase (ALT) (U/dl), alkaline phosphatase (ALP) (U/dl), and γ-glutamyltransferase (GGT) (U/l). Significant reduction in creatine kinase levels was observed in the Vivo-ME23 (Vivo-ME23) IV-treated *mdx* mice compared to the untreated mdx mice (*t*-test, $P \leq 0.05$, six mice each group). No significant differences were detected for other serum components between the two groups except for ALT, which showed elevated levels in the untreated *mdx* mice.

dystrophin in all skeletal muscles and ~10% in cardiac muscles (**Figure 4c**). As expected with the removal of single E23, the size of the induced dystrophin protein was similar to that of normal dystrophin (**Figure 4c**). Correct skipping of the targeted E23 was confirmed by RT-PCR (**Figure 4e**). Dystrophin expression was also restored in smooth muscles of blood vessels in the lung and intestines (**Figure 4f**). These results suggest that Vivo-Morpholino has a high efficiency in targeting the vascular system.

Repeated Vivo-ME23 treatment improves muscle pathology without obvious toxicity

Histologically, no increase in mononucleate infiltrates was observed in any muscles of the Vivo-ME23-treated *mdx* mice. The treatment reduced the number of degenerating fibers identified by immunostaining for the presence of immunoglobulin (Ig) within fibers, indicating a damaged (thus leaky) membrane (**Figure 5a**). The number of Ig-positive fibers ranged from 10 to 31 in the untreated *mdx* mice in the TA, quadriceps, and biceps, whereas only three or less fibers were Ig positive after the Vivo-ME23 treatment. The most direct evidence suggesting improvement of muscle pathology was the significant reduction in serum creatine kinase levels when compared to those of the untreated *mdx* mice, although still slightly higher than the normal range (**Figure 3f**). Percentage of centrally nucleated fibers was reduced in the muscles of the treated mice, but this is not statistically significant from the control *mdx*

mice (**Supplementary Figure S2**). This suggests that significant changes in centrally nucleated fiber of these muscles may require longer-term treatment or higher levels of dystrophin expression. However, pathological improvement in the diaphragm was clearly observed. Areas of degeneration indicated by increases in extracellular matrix, heavy infiltrates, and groups of small regenerating fibers were frequently observed in the untreated *mdx* mice but diminished in the diaphragm of treated mice (**Figure 5b**). No animal death occurred during the 10 weeks of repeated IV injections of Vivo-ME23 and the weight of treated mice remained similar to control mice (**Supplementary Figure S3**). Both liver and kidney were normal in histology without obvious inflammatory infiltrate and the levels of serum enzymes remained within the normal ranges (**Figure 3f** and **5b**).

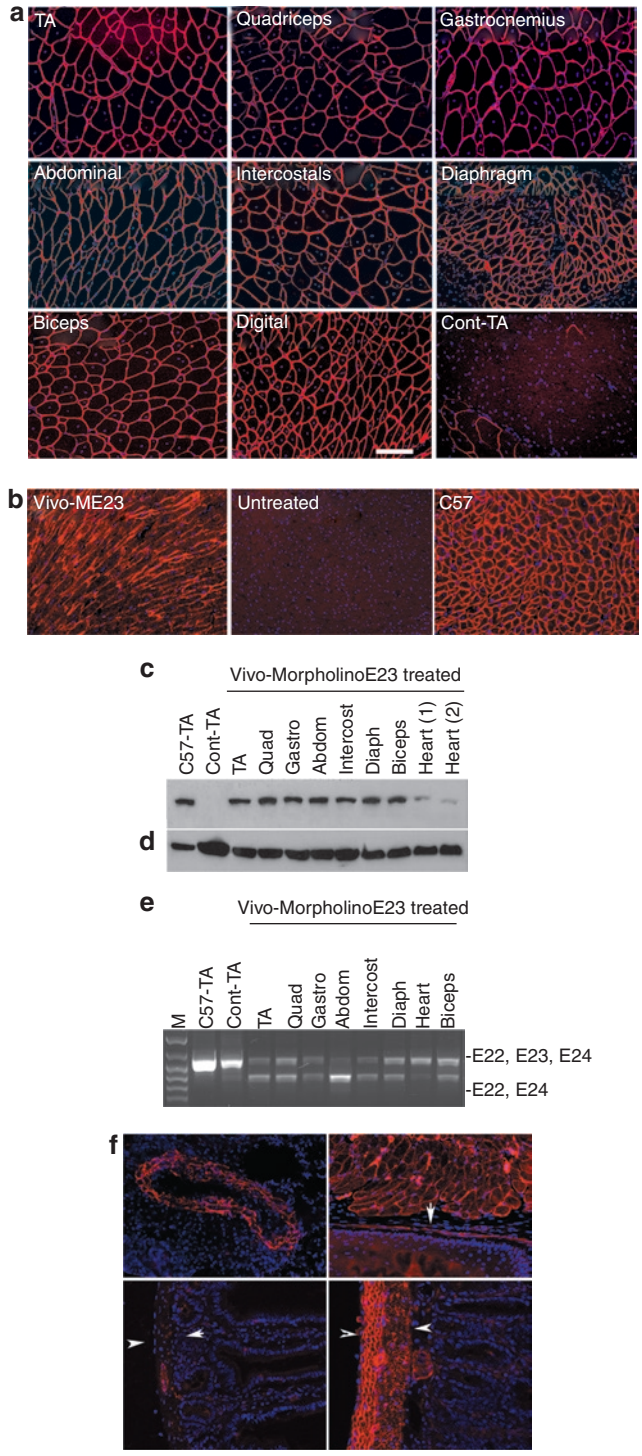

Lack of immune response to the Vivo-Morpholino

The cumulative effect of dystropohin expression after five systemic injections in nearly 3 months suggests that Vivo-Morpholino lacks immunuogenicity and permits repeated administration. This is consistent with the result with immunostaining for T lymphocytes. CD3-positive lymphocytes were present sporadically in almost all muscles of untreated *mdx* mice, including the diaphragm where considerable amount of muscle degeneration was apparent. The number of CD3-positive cells was only observed rarely in all the muscles of Vivo-Morpholino-treated mice (**Figure 5c**). We also looked for specific humoral immune responses in serum from mice after single and repeated administration of Vivo-Morpholino using a modified ELISA. The Vivo-Morpholino was used as an antigen coated on ELISA plates and probed with the serum from Vivo-Morpholino-treated and control mice for detection of specific antibodies. Only similar background signals were read with serum from all mice including normal *C57Bl/6* and untreated *mdx* mice (**Figure 5d**). This result is consistent with the improved pathology and reduced serum creatine kinase levels after Vivo-ME23 treatment.

DISCUSSION

Use of steric-block AONs to induce specific exon skipping has been among the most important advances toward a therapy for DMD. In our previous studies, we have shown that systemic administration of 2OMePS AONs to *mdx* mice were able to effectively skip E23, with its nonsense mutation, and thus elicit detectable amounts of dystrophin proteins in bodywide skeletal muscles.[25] However, 2OMePS AONs induced dystrophin at

Figure 4 Restoration of dystrophin expression after five times intravenous injection of 6 mg/kg Vivo-ME23. (**a**) skeletal and (**b**) cardiac muscles. (**a**) TA, tibialis anterior; Digital, right common extensor muscle of forelimb; Cont-TA, TA muscle from untreated *mdx* mouse. (**b**) Vivo-ME23, heart from Vivo-MorpholinoE23-treated *mdx* mouse; Untreated, heart from untreated *mdx* mouse; C57, heart from normal C57BL/6 mouse. Blue nuclear staining with 4′-6-Diamidino-2-phenylindole (DAPI). Bar = 100 µm. (**c**) Western blot shows ~50% and >10% of the normal levels of dystrophin in all skeletal muscles and cardiac muscles, respectively. C57-TA, TA muscle from normal C57BL/6 mouse (50% protein loading compared to the other samples); Cont-TA, TA muscle from untreated *mdx* mouse; Quad, quadriceps; Gastro, gastrocnemius; Abdom, abdominal muscle; intercost, intercostals; Diaph, diaphragm. (**d**) α-actin as loading controls. (**e**) Detection of exon 23 skipping by reverse transcriptase-PCR. Total RNA (100 ng from each sample) was used for amplification of dystrophin mRNA from exon 20 to exon 26. Lane M, size marker; Lanes represent the same muscle tissues as described in **c**. The upper 1,093-bp bands (indicated by E22, E23, E24) correspond to the normal dystrophin mRNA and the lower 880-bp bands (indicated by E22, E24) correspond to the mRNA with exon 23 skipped. (**f**) Restoration of dystrophin in the smooth muscles of an artery in the lung (top left), muscles of the esophagus (top right, arrow indicate the basal layer of the epithelium of the esophagus) and smooth muscles (layers between the two arrowheads) in small intestine of untreated *mdx* mouse (bottom left) and Vivo-ME23-treated *mdx* mouse (bottom right). Blue nuclear staining with DAPI.

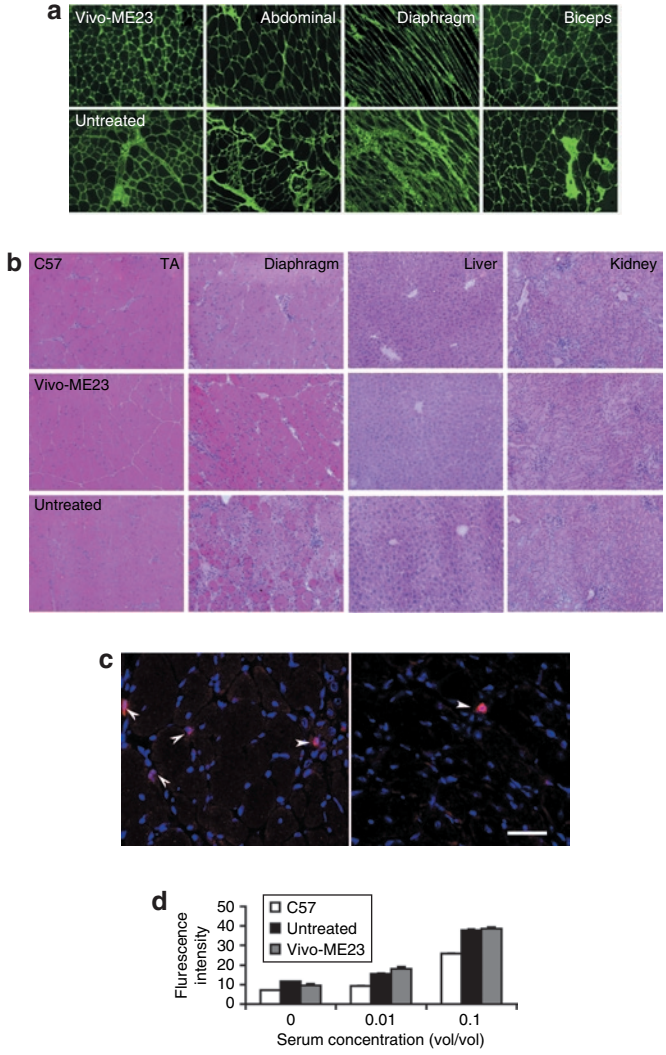

Figure 5 Examination of pathology and toxicity after Vivo-MorpholinoE23 (Vivo-ME23) treatment. (**a**) Staining for immunoglobulins (Igs) in muscles from Vivo-ME23-treated *mdx* mice (upper panel) and untreated *mdx* mice (untreated, lower panel). Mouse Igs were detected with Alexa 488 conjugated rabbit antimouse Igs (Molecular Probes). Considerable reduction is observed in the levels of Igs within the extracellular matrix, and no Ig-positive fiber is seen after the treatment of Vivo-ME23. (**b**) Hematoxylin and Eosin staining of cryosections in tibialis anterior (TA) muscles, diaphragms, kidneys, and livers from the normal C57BL/6 (C57) mice, untreated *mdx* (Untreated) mice, and Vivo-ME23-treated *mdx* mice. Areas of degeneration indicated by increase of extracellular matrix and heavy infiltrates with isolated small fibers are clearly seen in the diaphragm of control *mdx* mouse but not in that of treated-*mdx* mouse. No pathological change is observed in the kidneys and livers of the treated *mdx* mice. (**c**) Detection of T lymphocytes in diaphragms of untreated *mdx* (top left) and Vivo-ME23-treated *mdx* mouse (top right). Arrows indicate the T lymphocytes recognized by monoclonal antibody against mouse CD3; bar = 50 µm. (**d**) ELISA for antibodies against Vivo-ME23 in serum from the normal C57BL/6 (C57), untreated *mdx*, and Vivo-ME23-treated *mdx* mouse. Signals for the antibodies against Vivo-ME23 in the treated *mdx* mice are similar to the backgrounds detected in both control mice. 0, without mouse serum; 0.01 and 0.1, sample serum used in 1:100 and 1:10 dilution, respectively.

amounts considered not therapeutically significant in any muscle after repeated injections. Our follow-up study demonstrated that the same sequence synthesized as a Morpholino oligo significantly increased the efficiency of exon skipping over 2OMePS oligos when delivered intramuscularly. Furthermore, repeated injections of Morpholinos generated therapeutic levels of dystrophin expression in bodywide skeletal muscles, with improved muscle pathology.[15] The mechanism(s) of delivery of the unmodified Morpholino or 2OMePS oligos into muscle fibers *in vivo* and the difference in efficiency between the two chemistries are not clearly understood. However, AON-induced dystrophin expression was most conspicuous in myopathic areas of muscle, suggesting that AONs of both chemistries may enter the muscle fiber mainly through the partially damaged (leaky) membrane. The delivery of these two unmodified oligos is, therefore, likely a passive rather than an active transport process.[26,27] One of the major differences between the two chemistries is that 2OMePS AONs are, like natural oligonucleotides, negatively charged, whereas the Morpholino oligos are charge neutral. Therefore, the repulsion between the like charges of 2OMePS AONs and the molecules at the outer surface cell membrane would be expected to hinder efficient delivery of the AON into target cells. The charge-neutral Morpholino oligos, however, will have much less impediment to cell-surface contact and may thus enter muscle fibers more efficiently, particularly those with leaky membrane as seen in the dystrophic muscles. This, however, likely explains only partly the difference in antisense effect between the two chemistries. The dependence on muscle damage for effective delivery of neutral Morpholinos has an advantage of limiting the amount of AON entering nontargeted cells, thus diminishing possible side effects. However, this limitation presents a potential barrier for effective treatment of DMD.[15] Consistently, dystrophin expression induced by unmodified Morpholino was highly variable in all skeletal muscles, where asynchronous cycles of degeneration and regeneration result in fibers with different levels of membrane permeability. Considerable numbers of fibers remain dystrophin negative even after seven consecutive IV injections of 2 mg Morpholinos (per adult mouse, equivent to ~80 mg/kg body weight).[15] This model would predict that muscle fibers rescued earlier by Morpholino-induced exon skipping might have to re-enter a myopathic state before they could again be protected by further entry of antisense oligos. Such a requirement for recurring cycles of rescue and degeneration in treated muscles would severely limit the value of antisense therapy for DMD. Here we demonstrate that a dendrimeric octaguanidine delivery moiety can significantly improve the delivery efficiency of Morpholino oligos, with consequent induction of dystrophin expression in all muscle fibers of all skeletal muscles. Thus, rescue and maintenance of dystrophin expression can be achieved in both histologically normal and dystrophic muscles by regular injection of Vivo-Morpholinos.

Production of dystrophin in cardiac muscle becomes increasingly important for the life quality and longevity of DMD patients as improved multidisciplinary patient care reduces their mortality from other causes.[16,17] However, exon skipping in the cardiac muscle is still less efficient than in the skeletal muscle for reasons that are not yet understood. The guanidine groups in Vivo-Morpholinos are chemically similar to the active components of arginine, and poly-arginine-conjugated oligos have been suggested to enter target cells by proteoglycan-mediated endocytosis.[28] Therefore, it may be possible that the differences between these two types of muscles in the amount and distribution of the cell surface proteoglycans have a bearing on the difference in the

efficiency of exon skipping.[25,27] Other factors such as differences in blood circulation and clearance of AON from muscle fibers remain to be examined. Nevertheless, our finding that Vivo-Morpholinos are able to generate considerable amounts of dystrophin in cardiac muscle raise hopes of achieving rescue of cardiac function by antisense therapy.

The main barrier to a general successful application of oligonucleotide-mediated therapies has been the difficulties in achieving effective delivery of such compounds into target tissues *in vivo*.[1] Improved delivery of oligonucleotides has been reported with the use of cell-penetrating peptides.[20] More significantly, highly effective restoration of dystrophin expression in both skeletal and cardiac muscles in the dystrophic *mdx* mice has been achieved by Morpholino with specifically designed arginine-rich peptides.[19,21,22] However, the use of peptides risks a potential immune response to the conjugates, preventing repeated administrations that are essential for the treatment of DMD with oligomers. To evade immunogenicity of peptides, we explore the use of a delivery moiety assembled from a synthetic scaffold and multiple unnatural side chains, each containing guanidine head groups constructed on a dendrimeric core.[29] This special chemical feature eliminates the use of arginine-rich linear peptides that may be immunogenic. We expect that the synthetic nature of this delivery moiety is unlikely to be presented in a class 2 MHC dimmer to elicit a cytolytic immune response. This is supported by the fact that the number of lymphocytes and other mononucleates in the muscles of the Vivo-Morpholino-treated mice decreases in the course of the treatment. However, we are aware that such polymers may generate a humoral response that would limit regular administration to maintain functional levels of dystrophin in bodywide muscles. This prospect is not supported by our findings that dystrophin expression was sustained and enhanced after repeated injections of the Vivo-ME23 over 10 weeks, and no antibodies to the conjugate was detected. The principle of precaution together with the fact that immunogenicity varies greatly between species would argue for longer-term studies in other species.

In summary, our demonstration that a dendrimeric octa-guanidine delivery component enabled efficient delivery of Morpholino oligo to muscles bodywide, including the cardiac muscle, and that rescue of the dystrophin expression to functional levels in dystrophic *mdx* mice represent a significant step forward in our effort to overcome the barrier of effective systemic delivery of oligos. Perhaps also important is the finding that the dendrimeric octa-guanidine Morpholino is highly potent for tissue penetration. This was demonstrated by the effective targeting of abdominal muscles after IP injection. Cells even more than a dozen layers away from the peritoneal surface were effectively targeted to express dystrophin. Furthermore, all smooth muscles in the intestine are effectively targeted via IV delivery. The high potency in modulating RNAs and tissue penetration together provides the possibility of the Vivo-Morpholino targeting many tissues and vascular systems for the treatment of other diseases from cancer to viral infections.

MATERIALS AND METHODS

Animals, oligonucleotides, and delivery methods. The *mdx* mice aged 4–5 weeks were used with six mice in each group unless otherwise specified. The oligonucleotide sequence 5′-GGCCAAACCTCGGCTTACCTG AAAT-3′, against the boundary sequences of the exon and intron 23 of dystrophin gene (E23) was synthesized as Morpholino by (Gene Tools). Vivo-Morpholinos were made by conjugation of an unmodified Morpholino with a synthetic scaffold featuring eight guanidinium head groups.[29] Conjugation was carried out on the Morpholino synthesis column, followed by ammonolytic removal of the protecting groups and perguanidination. Vivo-Morpholino thus obtained was then purified on an Oasis HLB extraction cartridge (Waters, Milford, MA) (**Figure 1**). The Morpholinos were dissolved in saline and delivered directly or mixed with endoporter according to manufacturer's instruction (Gene Tools, Philomath, OR).

For intramuscular injections, 2 and 10 µg Morpholinos were used in 40 µl saline for each TA muscle. For IP or IV injection, ME23s were used in 100 µl saline. Mice were sacrificed at desired time points, and muscles were dissected immediately, snap frozen in liquid nitrogen-cooled isopentane and stored at −80 °C. The use of animals for experimental purpose was approved by Institutional Animal Care and Use Committee Carolinas Medical Center.

Antibodies and immunohistochemistry. Sections of 6 µm were cut from at least two thirds of muscle length of TA, quadriceps, biceps, and gastrocnemius at 100 µm intervals and at least 10 levels from all other muscles including heart, diaphragm, intercostals, and abdominal muscles at 100-µm intervals. The intervening muscle sections were collected either for western blot and RT-PCR analysis. The serial sections were stained with polyclonal rabbit antibody P7 and visualized by Alexa 594-conjugated goat antirabbit Igs (Molecular Probes, Carlsbad, CA). The number of dystrophin-positive fibers was counted from 1,000 fibers of each muscle sample, and six samples for each muscle were examined. Tissue endogenous Igs were detected with rabbit-antimouse Igs Alexa 488 and the maximum number of Ig-positive fiber in one cross-section was recorded in TA, quadracepts, and biceps that have defined cross-section area. Fluorescein isothiocyanate-labeled monoclonal antibody against mouse CD3 was obtained from EBioscience, San Diego, CA.

Protein extraction and western blot. The collected sections were grounded into powder and lysed with 200 µl protein extraction buffer as described previously.[25] The protein concentration was quantified by Protein Assay Kit (Bio-Rad, Irvine, CA). Proteins (50 µg for each sample unless specified otherwise) from muscles of normal *C57BL/6* mice (positive controls) and treated *mdx* mice were loaded onto a 6% polyacrylamide gel containing 0.2% sodium dodecyl sulfate and 10% glycerol. Samples were electrophoresed 4 hours at 150V, 4 °C and blotted onto nitrocellulose membrane 18 hours at 50 mA, 4 °C. The membrane was then washed and blocked with 5% skimmed milk and probed with monoclonal antibody NCL-DYS1 against dystrophin rod domain (Vector Labs, Burlingame, CA) overnight. The bound primary antibody was detected by horseradish peroxidase-conjugated goat antimouse IgG and ECL Western Blotting Analysis System (Perkin Elmer, Waltham, MA). The intensity of the bands obtained from the oligomer-treated *mdx* muscles was measured and compared with that obtained from normal muscles of *C57BL/6* mice (National Institutes of Health imaging software, Gel blotting macros).

RNA extraction and RT-PCR. The collected sections were homogenized in TRIzol (Invitrogen, Carlsbad, CA) by using an Ultra-Turrax homogenizer (Janke and Kunkel, Staufen, Germany). Total RNA was then extracted, and 100 ng of RNA template was used for a 50-µl RT-PCR with the Stratascript One-Tube RT-PCR System (Stratagene, Santa Clara, CA). The primer sequences for the RT-PCR were Ex20Fo 5′-CAGAATTCTGCCAATTGCTGAG-3′ and Ex26Ro 5′-TTCTTCAGCTTGTGTCATCC-3′ for amplification of mRNA from exons 20 to 26. Bands with the expected size for the transcript with E23 deleted were extracted and sequenced.

Measurement of serum creatine kinase and other components. Mouse blood was taken immediately after cervical dislocation and centrifuged at

1,500 rpm for 3 minutes. Serum was separated and stored at −80 °C. The level of serum components was determined by Charles Riverside Laboratories.

Central nucleated fiber counting. TA, quadriceps, and biceps muscles from *mdx* mice after repeated IV injections of ME23s were examined. The fibers were counted as centrally nucleated when one or more nuclei were not on the periphery of the fiber. Total of 1,000 fibers were assessed for each muscle sample ($n = 6$). Zeiss AxioPhot fluorescence microscope was used.

ELISA for serum antibody detection. ELISA plates were coated with 1 µg of Vivo-Morpholino, incubated at 4 °C overnight, washed, blocked with normal goat serum, and incubated with the serum from *C57BL/6* mice and the experimental mice in serial dilutions for 1 hour. The plates were then incubated for 1 hour with goat–antimouse Igs Alexa 488 (Invitrogen) for 30 minutes. The signal intensity was measured by the plate reader (Infinite F500; Tecan, Durham, NC).

SUPPLEMENTARY MATERIAL

Figure S1. Percentage of dystrophin positive fibers in muscles of *mdx* mice ($n = 6$) treated with morpholinos targeting dystrophin exson 23 (ME23).

Figure S2. Percentage of fibers with central nucleation.

Figure S3. Weight changes during the experimental period starting from the first day of repeated i.v. injection of 6 mg/kg Vivo-MorpholinoE23 (Day 0).

ACKNOWLEDGMENTS

This work was supported by Carolinas Medical Center, Charlotte, North Carolina; US Army Medical Research, Department of Defense (W81XWH-05-1-0616). We thank Herbert Bonkovsky, Cannon Research Center, Carolinas Medical Center, Charlotte, North Carolina, for critical comments of the manuscript.

REFERENCES

1. Blow, N (2007). Small RNAs: delivering the future. *Nature* **450**: 1117–1120.
2. Kumar, P, Wu, H, McBride, JL, Jung, KE, Kim, MH, Davidson, BL *et al.* (2007). Transvascular delivery of small interfering RNA to the central nervous system. *Nature* **448**: 39–43.
3. Sherratt, TG, Vulliamy, T, Dubowitz, V, Sewry, CA and Strong, PN (1993). Exon skipping and translation in patients with frameshift deletions in the dystrophin gene. *Am J Hum Genet* **53**: 1007–1015.
4. Dunckley, MG, Manoharan, M, Villiet, P, Eperon, IC and Dickson, G (1998). Modification of splicing in the dystrophin gene in cultured Mdx muscle cells by antisense oligoribonucleotides. *Hum Mol Genet* **7**: 1083–1090.
5. Mann, CJ, Honeyman, K, Cheng, AJ, Ly, T, Lloyd, F, Fletcher, S *et al.* (2001). Antisense-induced exon skipping and synthesis of dystrophin in the mdx mouse. *Proc Natl Acad Sci USA* **98**: 42–47.
6. Lu, QL, Mann, CJ, Lou, F, Bou-Gharios, G, Morris, GE, Xue, SA *et al.* (2003). Functional amounts of dystrophin produced by skipping the mutated exon in the mdx dystrophic mouse. *Nat Med* **9**: 1009–1014.
7. Dickson, G, Hill, V and Graham, IR (2002). Screening for antisense modulation of dystrophin pre-mRNA splicing. *Neuromuscul Disord* **12** (suppl. 1): S67–S70.
8. Aartsma-Rus, A, Bremmer-Bout, M, Janson, AA, den Dunnen, JT, van Ommen, GJ and van Deutekom, JC (2002). Targeted exon skipping as a potential gene correction therapy for Duchenne muscular dystrophy. *Neuromuscul Disord* **12** (suppl. 1): S71–S77.
9. England, SB, Nicholson, LV, Johnson, MA, Forrest, SM, Love, DR, Zubrzycka-Gaarn, EE *et al.* (1990). Very mild muscular dystrophy associated with the deletion of 46% of dystrophin. *Nature* **343**: 180–182.
10. Sakamoto, M, Yuasa, K, Yoshimura, M, Yokota, T, Ikemoto, T, Suzuki, M *et al.* (2002). Micro-dystrophin cDNA ameliorates dystrophic phenotypes when introduced into mdx mice as a transgene. *Biochem Biophys Res Commun* **293**: 1265–1272.
11. Winnard, AV, Klein, CJ, Coovert, DD, Prior, T, Papp, A, Snyder, P *et al.* (1993). Characterization of translational frame exception patients in Duchenne/Becker muscular dystrophy. *Hum Mol Genet* **2**: 737–744.
12. Mirabella, M, Galluzzi, G, Manfredi, G, Bertini, E, Ricci, E, De Leo, R *et al.* (1998). Giant dystrophin deletion associated with congenital cataract and mild muscular dystrophy. *Neurology* **51**: 592–595.
13. Lu, QL, Morris, GE, Wilton, SD, Ly, T, Artem'yeva, OV, Strong, P *et al.* (2000). Massive idiosyncratic exon skipping corrects the nonsense mutation in dystrophic mouse muscle and produces functional revertant fibers by clonal expansion. *J Cell Biol* **148**: 985–996.
14. van Deutekom, JC, Janson, AA, Ginjaar, IB, Frankhuizen, WS, Aartsma-Rus, A, Bremmer-Bout, M *et al.* (2007). Local dystrophin restoration with antisense oligonucleotide PRO051. *N Engl J Med* **357**: 2677–2686.
15. Alter, J, Lou, F, Rabinowitz, A, Yin, H, Rosenfeld, J, Wilton, SD *et al.* (2006). Systemic delivery of morpholino oligonucleotide restores dystrophin expression bodywide and improves dystrophic pathology. *Nat Med* **12**: 175–177.
16. Eagle, M, Bourke, J, Bullock, R, Gibson, M, Mehta, J, Giddings, D *et al.* (2007). Managing Duchenne muscular dystrophy—the additive effect of spinal surgery and home nocturnal ventilation in improving survival. *Neuromuscul Disord* **17**: 470–475.
17. Wagner, KR, Lechtzin, N and Judge, DP (2007). Current treatment of adult Duchenne muscular dystrophy. *Biochim Biophys Acta* **1772**: 229–237.
18. Fletcher, S, Honeyman, K, Fall, AM, Harding, PL, Johnsen, RD, Steinhaus, JP *et al.* (2007). Morpholino oligomer-mediated exon skipping averts the onset of dystrophic pathology in the mdx mouse. *Mol Ther* **15**: 587–1592.
19. Wu, B, Moulton, HM, Iversen, PL, Jiang, J, Li, J, Spurney, CF *et al.* (2008). Effective rescue of dystrophin improves cardiac function in dystrophin-deficient mice by a modified morpholino oligomer. *Proc Natl Acad Sci USA* **105**: 14814–14819.
20. Yin, H, Moulton, HM, Seow, Y, Boyd, C, Boutilier, J, Iverson, P *et al.* (2008). Cell-penetrating peptide-conjugated antisense oligonucleotides restore systemic muscle and cardiac dystrophin expression and function. *Hum Mol Genet* **17**: 3909–3918.
21. Jearawiriyapaisarn, N, Moulton, HM, Buckley, B, Roberts, J, Sazani, P, Fucharoen, S *et al.* (2008). Sustained dystrophin expression induced by peptide-conjugated morpholino oligomers in the muscles of mdx mice. *Mol Ther* **16**: 1624–1629.
22. Futaki, S, Nakase, I, Suzuki, T, Youjun, Z and Sugiura, Y (2002). Translocation of branched-chain arginine peptides through cell membranes: flexibility in the spatial disposition of positive charges in membrane-permeable peptides. *Biochemistry* **41**: 7925–7930.
23. Hoffman, EP, Morgan, JE, Watkins, SC and Partridge, TA (1990). Somatic reversion/suppression of the mouse mdx phenotype *in vivo*. *J Neurol Sci* **99**: 9–25.
24. Sicinski, P, Geng, Y, Ryder-Cook, AS, Barnard, EA, Darlison, MG and Barnard, PJ (1989). The molecular basis of muscular dystrophy in the mdx mouse: a point mutation. *Science* **244**: 1578–1580.
25. Lu, QL, Rabinowitz, A, Chen, YC, Yokota, T, Yin, H, Alter, J *et al.* (2005). Systemic delivery of antisense oligoribonucleotide restores dystrophin expression in body-wide skeletal muscles. *Proc Natl Acad Sci USA* **102**: 198–203.
26. Kurreck, J (2003). Antisense technologies. Improvement through novel chemical modifications. *Eur J Biochem* **270**: 1628–1644.
27. Summerton, J and Weller, D (1997). Morpholino antisense oligomers: design, preparation, and properties. *Antisense Nucleic Acid Drug Dev* **7**: 187–195.
28. Abes, S, Moulton, HM, Clair, P, Prevot, P, Youngblood, DS, Wu, RP *et al.* (2006). Vectorization of morpholino oligomers by the (R-Ahx-R)4 peptide allows efficient splicing correction in the absence of endosomolytic agents. *J Control Release* **116**: 304–313.
29. Li, YF and Morcos, PA (2008). Design and synthesis of the dendritic molecular transporter that achieves efficient *in vivo* delivery of morpholino antisense oligo. *Bioconjug Chem* **19**: 1464–1470.